

JOURNAL OF THE AMERICAN CHEMICAL SOCIETY

Catalysis of Phosphoryl Transfer from ATP by Amine Nucleophiles

Suzanne J. Admiraal and Daniel Herschlag*

Contribution from the Department of Biochemistry, Beckman Center B400, Stanford University, Stanford, California 94305-5307

Received March 19, 1999

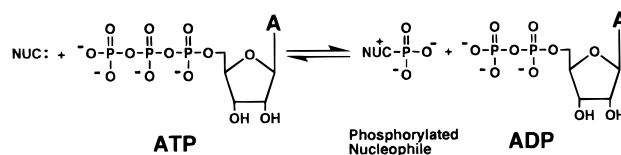
Abstract: Phosphoryl transfer from the high-energy phosphate donor ATP is ubiquitous in biological chemistry, and nitrogen nucleophiles, especially histidine, often serve as *in vivo* acceptors of the γ -phosphate of ATP. Nevertheless, nonenzymatic reactions of ATP with amines have not previously been characterized. We have therefore examined phosphoryl transfer from ATP to amines to provide a basis for understanding the analogous enzymatic reactions, and we have compared the rates of these reactions to the rates with oxygen nucleophiles in order to assess whether intrinsically higher reactivities of nitrogen nucleophiles could cause them to be favored over oxygen nucleophiles in covalent catalysis of phosphoryl transfer by enzymes. Reactions of amine nucleophiles are 30–100-fold faster than reactions of oxygen nucleophiles at physiological temperatures. Thus, the reactivity of amines, in addition to thermodynamic and evolutionary factors, may have played a role in the selection of nitrogen nucleophiles for use in biological phosphoryl-transfer reactions. In the course of these studies, the reaction of fluoride ion with ATP tetraanion was also observed. Surprisingly, the rate constant for the reaction of fluoride ion with ATP is similar to rate constants for reactions of uncharged amine and oxygen nucleophiles with ATP, providing no support for proposals that reactions of ATP and other phosphoryl anions with anionic nucleophiles are prevented by electrostatic repulsion in aqueous solution.

Introduction

Enzymes that catalyze phosphoryl transfer from ATP include ATPases that use a water nucleophile to attack ATP, small molecule kinases that use metabolites as nucleophiles, and protein kinases that undergo nucleophilic reaction with ATP at amino acid side chains. In molecular detail, all of these enzymatic reactions reduce to the phosphoryl group transfer diagrammed in Scheme 1. The nucleophile that attacks ATP at the γ -phosphate is most commonly an oxygen nucleophile, such as an alcohol or a carboxylate. Products of the reaction are an ADP leaving group and a phosphorylated nucleophile.

Some phosphoryl-transfer enzymes utilize a nitrogen nucleophile to attack ATP. Nucleoside diphosphate kinase (NDPK),¹

Scheme 1



guardian of the cell's NTP balance, and the histidine kinases of histidyl-aspartyl phosphorelays, activators of a broad range of cellular responses to environmental signals in both prokaryotes and eukaryotes,² are examples of such enzymes. In each case, a nitrogen of an active site histidine is the nucleophile that attacks ATP to produce a phosphorylated histidyl enzyme.

(1) Abbreviations: NDPK, nucleoside diphosphate kinase; NTP, nucleoside triphosphate; NDP, nucleoside diphosphate; PNPP, *p*-nitrophenyl phosphate; Im, imidazole; ImP, imidazole phosphate; P_i, inorganic phosphate; PAGE, polyacrylamide gel electrophoresis.

* To whom correspondence should be addressed. Phone: 650-723-9442. Fax: 650-723-6783. E-mail: herschla@cmgm.stanford.edu.

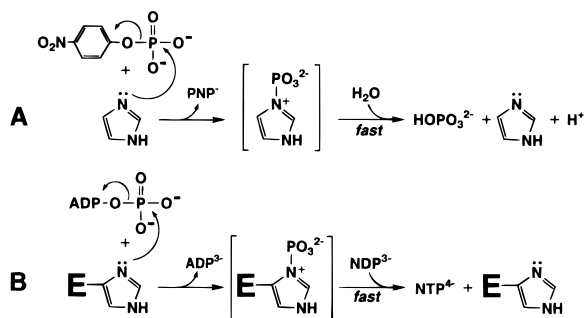


Figure 1. Nucleophilic catalysis by nitrogen nucleophiles? (A) Nucleophilic catalysis of PNPP²⁻ hydrolysis by Im is observed. Im reacts initially as the attacking nucleophile, and the ImP intermediate (in brackets) is subsequently hydrolyzed to form P_i and regenerate Im. The rate constant for Im reaction with PNPP²⁻ is 200-fold larger than the rate constant for direct water reaction with PNPP²⁻,⁴ and the subsequent hydrolysis of ImP is fast relative to PNPP²⁻ breakdown. Thus, Im functions as a nucleophilic catalyst. (B) Model for possible nucleophilic catalysis of NTP interconversion in the NDPK reaction. His 122 acts initially as the attacking nucleophile toward ATP, and the phosphorylated NDPK intermediate (in brackets) subsequently reacts with an NDP to form the corresponding NTP and regenerate free NDPK.

The modified enzyme is subsequently dephosphorylated: NDPK uses a different NDP as a nucleophile to complete its interconversion of two NTPs, and phosphorylated histidine kinases are attacked by an aspartate of a partner response regulator, thereby transmitting their phosphorylation signal to a second protein.

We were interested in possible chemical rationales for the use of nitrogen nucleophiles in enzyme-catalyzed phosphoryl-transfer reactions. One proposal is that amines act as nucleophilic catalysts, speeding the overall transfer of phosphate to an oxygen nucleophile by intermediate phosphorylation of nitrogen.³ This model arises from the differential reactivities observed for oxygen and nitrogen nucleophiles for their respective reactions with phosphate esters. For example, nucleophilic attack upon PNPP²⁻ by Im occurs 200-fold faster than attack by water.⁴ The ImP intermediate formed upon reaction with Im is kinetically more labile than the PNPP substrate and thermodynamically less stable than the hydrolysis product, P_i.⁵ Thus, Im functions as a nucleophilic catalyst of the overall hydrolysis of PNPP (Figure 1A). Extension of the nucleophilic catalysis model to ATP and enzymes such as NDPK posits that the potentially slow reaction of an oxygen of NDP with ATP is substituted by two intrinsically faster reactions: a nitrogen of histidine attacking ATP, followed by the NDP attacking the phosphorylated histidyl enzyme (Figure 1B). However, reactions of Im and other amines with ATP had never been observed in solution, so there was no experimental basis for the nucleophilic catalysis model for ATP. We therefore set out to test the possibility that nitrogen nucleophiles provide a kinetic advantage over oxygen nucleophiles that could be exploited enzymatically.

(2) Appleby, J. L.; Parkinson, J. S.; Bourret, R. B. *Cell* **1996**, *86*, 845–848. Brown, J. M.; Firtel, R. A. *Curr. Biol.* **1998**, *8*, R662–R665. Egger, L. A.; Park, H.; Inouye, M. *Genes Cells* **1997**, *2*, 167–184. Loomis, W. F.; Shaulsky, G.; Wang, N. *J. Cell. Sci.* **1997**, *110*, 1141–1145.

(3) Jencks, W. P. *Catalysis in Chemistry and Enzymology*; Dover: New York, 1987; pp 107–111. Abelson, R. H.; Frey, P. A.; Jencks, W. P. *Biochemistry*; Jones and Bartlett: Boston, 1992; pp 295–328.

(4) Kirby, A. J.; Jencks, W. P. *J. Am. Chem. Soc.* **1965**, *87*, 3209–3216.

(5) The rate constant for hydrolysis of ImP⁻ is $2 \times 10^{-5} \text{ M}^{-1} \text{ min}^{-1}$ at 40.1 °C (ref 8), 10³-fold faster than the rate constant of $2 \times 10^{-8} \text{ M}^{-1} \text{ min}^{-1}$ for hydrolysis of PNPP²⁻ at 39 °C (ref 4). An equilibrium constant of $4 \times 10^5 \text{ M}$ has been calculated for the hydrolysis of ImP⁻, 10⁴-fold larger than the equilibrium constant of 55 M for hydrolysis of HOPO₃²⁻ (ref 14).

We have detected reactions of amines with ATP and have demonstrated that amine nucleophiles do, indeed, catalyze phosphoryl transfer from ATP in solution. These results suggest that amine reactivity could be one component that has favored the participation of nitrogen nucleophiles in some phosphoryl-transfer reactions. In the course of this study, we have also detected reaction of fluoride ion with ATP tetraanion.

Experimental Section

Materials. Pyridine, 3-picoline, 4-picoline, potassium fluoride, sodium fluoride, tetramethylammonium fluoride, disodium fluorophosphate, and phosphorus oxychloride were from Aldrich and were the highest purity available. Im and PNPP were obtained from Baker and Sigma, respectively. Ultrapure ATP was from Pharmacia. Unpurified [γ -³²P]ATP was obtained from Amersham, but multiple radioactive bands were detected when the radiolabeled nucleotide was analyzed by PAGE and exposed to film (Kodak). Radiolabeled ATP was therefore separated from contaminants by electrophoresis on 15% polyacrylamide gels and eluted with water prior to use in experiments. Water was doubly distilled from an all-glass apparatus.

³²P-Labeled ImP was synthesized enzymatically using a point mutant of *Dictyostelium discoideum* NDPK, H122G. This mutant lacks the histidine nucleophile of the wild-type enzyme, so that addition of exogenous Im and [γ -³²P]ATP to a reaction mixture containing H122G results in production of ³²P-labeled ImP.⁶ Radiolabeled ImP was separated from the substrates and the ADP product by electrophoresis on 15% polyacrylamide gels and eluted with water prior to use in reactions.

Reactions of ATP⁴⁻. Reactions of ATP with amines were performed at 95 °C in 30 mM sodium pyrophosphate buffer, pH 8.3, and $I = 0.5$ (NaCl). Reaction pH was varied to confirm that the pH-independent reaction of ATP⁴⁻ was followed under these conditions. Reactions contained 0–0.5 M sodium fluoride and 0–1 M amine and were initiated by addition of 100 μM ATP (final concentration) containing trace [γ -³²P]ATP. Aliquots were removed at 3–5 specified times and quenched at 0 °C. Radiolabeled substrate (ATP) and products (P_i and fluorophosphate) were separated by electrophoresis on 15% polyacrylamide gels, and their relative amounts at each time point were quantitated with a Molecular Dynamics PhosphorImager. Observed rate constants (k_{obs}) were obtained from exponential fits using Kaleidagraph (Abelbeck Software) and typically gave $R \geq 0.99$. Values of k_{obs} and [FPO₃]/[HOPO₃] obtained from the analysis are listed in Table 1 in the Results and were reproducible to $\pm 5\%$ and $\pm 10\%$, respectively. The [FPO₃]/[HOPO₃] ratios were constant throughout individual time courses, indicating that no secondary reactions involving the reaction products were occurring. ³¹P NMR chemical shifts and a phosphorus–fluorine coupling constant ($J_{\text{P-F}} = 865 \text{ Hz}$)⁷ consistent with the expected P_i and fluorophosphate products were observed in analogous nonradioactive reactions.

When reactions containing Im were performed as described above but at pH > 11 (50 mM sodium phosphate or sodium carbonate buffer), an ImP product was detected on polyacrylamide gels. The formation of ImP provides direct support for the interpretation that the increased k_{obs} and increased formation of fluorophosphate with increasing Im result from nucleophilic attack of Im on ATP (see Results). The ability to detect ImP product at high pH presumably results from accumulation of ImP²⁻, which is extremely stable relative to ImP⁻ because its hydrolysis would involve anionic Im as a leaving group.⁸ Even though the pK_a of ImP is considerably less than 11, the higher pH is necessary to slow ImP hydrolysis sufficiently such that the breakdown of product ImP is slower than the breakdown of the ATP substrate.

Reactions of ATP and amines were performed at 65, 75, and 85 °C, under the reaction conditions described above (pH 8.3) but without added fluoride. Second-order rate constants for the reactions of water with ATP⁴⁻ were determined from k_{obs} in the absence of amines divided

(6) Admiraal, S. J.; Schneider, B.; Meyer, P.; Janin, J.; Véron, M.; Deville-Bonne, D.; Herschlag, D. *Biochemistry* **1999**, *38*, 4701–4711.

(7) Vogel, H. J.; Bridger, W. A. *Biochemistry* **1982**, *21*, 394–401.

(8) Lloyd, G. J.; Cooperman, B. S. *J. Am. Chem. Soc.* **1971**, *93*, 4883–4889.

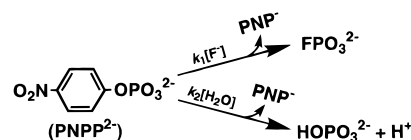
by 55 M water, and second-order rate constants for the reactions of amines were obtained from the slopes of plots of k_{obs} as a function of amine concentration, as recorded in Table 3 in the Results. 2,6-Dimethylpyridine, a sterically hindered pyridyl derivative, did not increase the observed reaction rate, suggesting that the rate enhancements observed in reactions containing nucleophilic pyridines do not result from solvent effects.⁹

Reactions of *N*-Phosphorylated Amines. Aqueous solutions of *N*-phosphorylated pyridines were prepared as described previously.¹⁰ Briefly, phosphorylation of pyridine, 3-picoline, and 4-picoline was effected by the forceful injection with a pipettor of 150 μL of a solution containing the pyridine at a concentration of 0.15 M in 2.3 M NaOH into a microcentrifuge tube containing $\sim 9 \mu\text{L}$ (4 equiv) of POCl_3 . All solutions were at 0 °C. These components were mixed for ~ 3 s by vigorous pipetting, and 3–5 μL of this synthesis mixture was immediately added to a quartz cuvette containing 1 mL of 30 mM sodium pyrophosphate buffer, pH 8.3, and 0–0.5 M sodium fluoride at $I = 0.5$ (NaCl). Disappearance of the phosphorylated compounds was monitored at 25 °C by following the decrease in absorbance at 260 nm for phosphorylated pyridine, 263 nm for phosphorylated 3-picoline, and 252 nm for phosphorylated 4-picoline. No catalysis by the pyrophosphate buffer was observed, and the pH was confirmed at the end of each reaction. Observed rate constants (k_{obs}) were obtained from exponential fits using Kaleidagraph (Abelbeck Software) and typically gave $R \geq 0.99$. Apparent second-order rate constants for reactions of water with the phosphorylated pyridines were determined from k_{obs} in the absence of fluoride divided by 55 M water, and apparent second-order rate constants for reactions of fluoride were obtained from the slopes of plots of k_{obs} as a function of fluoride concentration. These rate constants are apparent because they were measured under reaction conditions that match the ATP measurements described above and are not necessarily pH-independent. However, the apparent rate constants determined for hydrolysis and fluorolysis of phosphorylated pyridine and phosphorylated 4-picoline are within 20% of previously measured second-order rate constants,¹¹ suggesting that these apparent values do represent the actual second-order rate constants.

Reactions of ³²P-labeled ImP with water and fluoride were monitored at 75 °C. Reaction mixtures contained 30 mM sodium pyrophosphate buffer, pH 8.3, and 0–0.5 M sodium fluoride at $I = 0.5$ (NaCl). Reactions were initiated by the addition of trace ³²P-labeled ImP, and aliquots were removed at specified times and quenched at 0 °C. Radiolabeled substrate (ImP) and products (P_i and fluorophosphate) were separated by electrophoresis on 15% polyacrylamide gels, and their relative amounts at each time point were quantitated with a Molecular Dynamics PhosphorImager. Observed rate constants (k_{obs}) were obtained from exponential fits using Kaleidagraph (Abelbeck Software) and typically gave $R \geq 0.99$. The apparent relative rate constant for reaction of ImP with fluoride, $k_{\text{rel}}^{\text{F}^- \text{, ImP}}$, was determined from $[\text{FPO}_3]/[\text{HOPO}_3]$ product ratios, as described in the Results. This rate constant is apparent because it was measured under reaction conditions that match the ATP measurements described above; it is not expected to be pH-independent.

Reaction of Fluoride with PNPP^{2-} . Reaction mixtures containing 15 mM PNPP and 1–3 M potassium fluoride were adjusted to pH 12 or 13 with KOH and incubated at 95 °C. Aliquots were removed at specified time points and analyzed by ³¹P NMR. Chemical shifts and a phosphorus–fluorine coupling constant ($J_{\text{P-F}} = 865 \text{ Hz}$)⁷ consistent with P_i and fluorophosphate products were observed. The product ratio $[\text{FPO}_3]/[\text{HOPO}_3]$ was obtained from integration of the peaks corresponding to P_i and fluorophosphate and was used to calculate the rate constant for reaction of fluoride relative to that for reaction with water ($k_{\text{rel}}^{\text{F}^- \text{, PNPP}}$), according to Scheme 2. Data from five samples were averaged, giving $k_{\text{rel}}^{\text{F}^- \text{, PNPP}} = 2 \pm 1$. Values of k_{rel} were independent of pH, and the P_i produced is from attack by water rather than hydroxide

Scheme 2

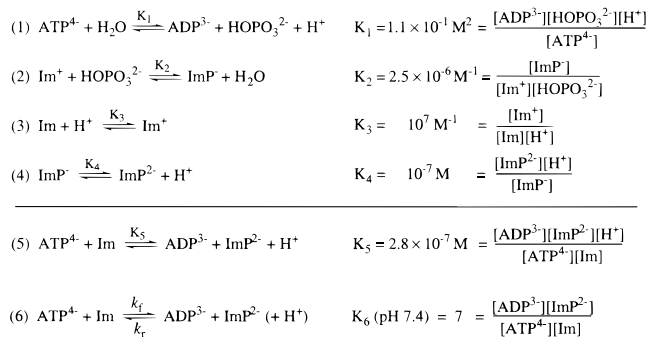


$$k_{\text{rel}}^{\text{F}^- \text{, PNPP}} = \frac{k_1}{k_2} = \frac{[\text{FPO}_3]}{[\text{HOPO}_3]} \times \frac{[\text{H}_2\text{O}]}{[\text{F}]}$$

ion in the pH regime investigated.⁴ Thus, reactions of PNPP^{2-} with H_2O and fluoride were monitored.

Free Energy Reaction Profiles. The free energy profiles shown in Figure 4 in the Discussion were constructed from equilibrium and rate constants at pH 7.4 and 25 °C. Standard states of 1 M were used for all reactants, except for the proton concentration, which was fixed at 4×10^{-8} M for the standard state of pH 7.4.¹² Equilibrium and rate constants were converted to ΔG values using $\Delta G = -RT \ln K$ and $\Delta G^\ddagger = -RT \ln[hk/(k_{\text{B}}T)]$, respectively, in which R is the gas constant, T is temperature in kelvin (298 K), h is Planck's constant, and k_{B} is the Boltzmann constant.

The free energy profile for reaction of ATP and NDP through an intermediate, ImP, was constructed as follows. The equilibrium for hydrolysis of ATP at pH 7.4 ($K_{\text{eq}} = 2.8 \times 10^6 \text{ M}$)¹³ was converted to the pH-independent equilibrium of eq 1 by explicitly including the proton. Equation 2 is the inverse of ImP hydrolysis, and K_2 is consequently the inverse of $K_{\text{eq}} = 4 \times 10^5 \text{ M}$ for ImP hydrolysis.¹⁴ The $\text{p}K_{\text{a}}$ values of both Im and ImP are ~ 7 ,⁸ so the predominant ionic species at pH 7.4 are Im and ImP^{2-} ; eqs 3 and 4 are included in the analysis to account for these ionizations. Equations 1–4 were combined



to give the pH-independent equilibrium of eq 5, and fixing the proton concentration at 4×10^{-8} M gives eq 6, the equilibrium for reaction of ATP and Im to produce ADP and ImP at pH 7.4.¹² The forward rate constant, k_f , of $3.7 \times 10^{-9} \text{ M}^{-1} \text{ s}^{-1}$ for eq 6 is from this work. The value of $k_r = 5.3 \times 10^{-10} \text{ M}^{-1} \text{ s}^{-1}$ was then calculated from this rate constant and $K_6 = k_f/k_r$ (eq 6). ATP and NTP were assumed to be thermodynamically and kinetically equivalent for the purposes of this analysis, so the reaction of NDP and ImP to produce NTP and Im is energetically the reverse of eq 6; the same rate and equilibrium constants described were therefore used to complete the right half of the free energy profile.

The free energy profile for intermediate phosphorylation of an alcohol was constructed analogously, using rate and equilibrium constants for methanol (ROH). Equation 1 from above for the pH-independent equilibrium for hydrolysis of ATP is repeated below for clarity. Equation 7 is the inverse of methyl phosphate (ROPO_3^{2-}) hydrolysis, and K_7 is consequently the inverse of $K_{\text{eq}} = 44 \text{ M}$ for

(12) Abeles, R. H.; Frey, P. A.; Jencks, W. P. *Biochemistry*; Jones and Bartlett: Boston, 1992; pp 245–249.

(13) Jencks, W. P. In *Handbook of Biochemistry and Molecular Biology*, 3rd ed.; Fasman, G. D. Ed.; CRC Press: Cleveland, OH, 1976; Vol. 1, pp 296–304.

(14) Herschlag, D.; Jencks, W. P. *J. Am. Chem. Soc.* **1990**, *112*, 1942–1950.

(15) Admiraal, S. J.; O'Brien, P.; Herschlag, D., unpublished results.

(9) Kirby, A. J.; Varvoglis, A. G. *J. Chem. Soc. (B)* **1968**, 135–141.

(10) Skoog, M. T.; Jencks, W. P. *J. Am. Chem. Soc.* **1984**, *106*, 7597–7606.

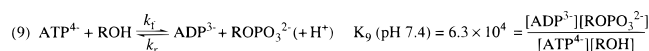
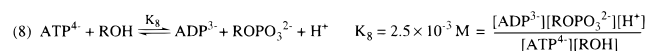
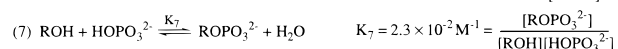
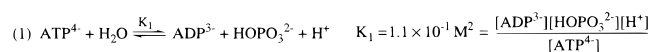
(11) Herschlag, D.; Jencks, W. P. *J. Am. Chem. Soc.* **1987**, *109*, 4665–4674. Herschlag, D.; Jencks, W. P. *J. Am. Chem. Soc.* **1990**, *112*, 2, 1951–1956.

Table 1. Reactions of ATP with Amine Nucleophiles^a

amine	pK _a ^b	[amine], M ^c	[F ⁻], M	10 ⁵ k _{obs} , s ⁻¹	[FPO ₃]/[HOPO ₃]	k _{rel} ^{amine d}	average k _{rel} ^{amine e}	10 ⁶ k _{amine} , M ⁻¹ s ^{-1 f}
none		0	0.0	6.0				
			0.25	6.0	0.008			
			0.5	5.8	0.014			
pyridine	5.5	0.31	0.0	6.0			6.8 ± 1.3	7.5
			0.25	6.2	0.011	7.4		
			0.5	6.1	0.019	4.9		
		0.62	0.0	6.7				
			0.25	6.5	0.015	8.0		
			0.5	6.3	0.027	7.0		
3-picoline	6.0	0.16	0.0	6.1			6.2 ± 3.1	6.8
			0.25	6.0	0.010	7.8		
			0.5	5.8	0.016	2.5		
		0.33	0.0	6.5				
			0.25	6.3	0.014	9.5		
			0.5	6.2	0.021	5.1		
4-picoline	6.3	0.16	0.0	6.1			5.6 ± 2.0	6.2
			0.25	6.0	0.010	5.7		
			0.5	6.0	0.017	3.1		
		0.33	0.0	6.3				
			0.25	6.2	0.015	7.9		
			0.5	6.2	0.024	5.7		
imidazole	7.0	0.50	0.0	6.7			7.4 ± 0.6	8.1
			0.25	6.5	0.014	8.2		
			0.5	6.2	0.025	6.9		
		1.0	0.0	7.2				
			0.25	7.2	0.019	7.5		
			0.5	6.8	0.035	7.1		

^a At 95 °C, 30 mM sodium pyrophosphate, pH 8.3, and *I* = 0.5 (NaCl). ^b From Jencks, W. P.; Regenstein, J. In *Physical and Chemical Data. Handbook of Biochemistry and Molecular Biology*, 3rd ed.; Fasman, G. D., Ed.; CRC Press: Cleveland, OH, 1976; Vol. 1, pp 305–351. ^c Concentrations were adjusted for self-association using *K*_{as} values of 0.5 M⁻¹ for pyridine, 3 M⁻¹ for 3-picoline, and 3 M⁻¹ for 4-picoline (ref 10). ^d Calculated according to the equation derived in Scheme 3 using *k*_{rel}^{F⁻-ATP} = 1.6, [H₂O] = 55 M, values of *k*_{rel}^{F⁻-AmP} from Table 2, and [amine], [F⁻], and [FPO₃]/[HOPO₃] from this table. ^e Errors represent one standard deviation from the mean. ^f Calculated from *k*_{rel}^{amine} = *k*_{amine}/*k*_{HOH} and *k*_{HOH} = 1.1 × 10⁻⁶ M⁻¹ s⁻¹; *k*_{HOH} is *k*_{obs} in the absence of amine divided by 55 M.

hydrolysis.¹⁵ Equations 1 and 7 were combined to give the pH-



independent equilibrium of eq 8. Accounting for the proton concentration (4×10^{-8} M) gives eq 9, the equilibrium for reaction of ATP and methanol to produce ADP and methyl phosphate at pH 7.4.¹² The forward rate constant, *k*_f, of 1.2×10^{-10} M⁻¹ s⁻¹ for eq 9 was obtained from the rate constant for reaction of ATP⁴⁻ with water (1.1×10^{-10} M⁻¹ s⁻¹, this work) and *k*_{rel} = 1.1 for reaction of methanol relative to water with ATP⁴⁻.¹⁶ The value of *k*_r = 1.9×10^{-15} M⁻¹ s⁻¹ was then calculated from *k*_f and *K*₉ = *k*_f/*k*_r (eq 9). ATP and NTP were assumed to be thermodynamically and kinetically equivalent for the purposes of this analysis, so the reaction of NDP and methyl phosphate to produce NTP and methanol is energetically the reverse of eq 9. The rate and equilibrium constants described above, therefore, allowed the remainder of the free energy profile to be completed.

Results

Reactions of Amine Nucleophiles with ATP? Nonenzymatic reactions of ATP with nitrogen nucleophiles have not previously been described. Amines must compete for reaction with 55 M water, and we postulated that this competition accounted for prior failure to observe these reactions. Thus, even if the amines were significantly more reactive than water on a molar basis,

there might be little or no detectable increase in the observed rate of ATP disappearance in the presence of amines. Indeed, the observed rate of ATP disappearance increased only slightly as a function of amine concentration at 95 °C (*k*_{obs}, Table 1). We were reluctant to interpret small rate increases in terms of nucleophilic attack because amine addition introduces changes in solvent composition, potentially leading to rate anomalies induced by solvent effects.

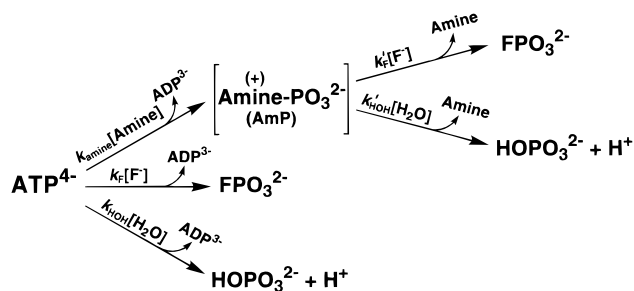
For reactions of ATP with alcohol nucleophiles, product analysis of the resulting alkyl phosphates allowed determination of the rates of alcohol attack, despite the similarity of these rates to that for attack by water.¹⁶ However, phosphorylated amines are less stable than ATP and do not accumulate during the reactions, so direct product analysis was not possible.¹⁷ An alternative strategy was therefore attempted: indirect trapping of the phosphorylated amine product via reaction with fluoride to form fluorophosphate (Scheme 3). Fluoride is known to react with phosphorylated amines,¹⁸ and fluorophosphate is stable under the reaction conditions used (data not shown). We presumed, and later confirmed, that fluoride would react more slowly with ATP than with the phosphorylated amines. This would then result in an increase in fluorophosphate product upon addition of amines, with the increase corresponding quantitatively to the extent of reaction between ATP and amine. Fluoride was previously used to trap phosphorylated amine intermediates resulting from nucleophilic attack of amines upon the dianions of acetyl phosphate and 2,4-dinitrophenyl phosphate.¹⁸

The results in Figure 2 illustrate the viability of this strategy for reactions of ATP. The radiolabeled ATP substrate and P_i

(17) Phosphorylated amines did not accumulate, except for ImP in reactions performed at high pH. See Experimental Section.

(18) Kirby, A. J.; Varvoglis, A. G. *J. Chem. Soc. (B)* **1968**, 135–141. DiSabato, G.; Jencks, W. P. *J. Am. Chem. Soc.* **1961**, 83, 4393–4400.

Scheme 3



$$k_{\text{rel}}^{\text{F,ATP}} = \frac{k_{\text{F}}}{k_{\text{HOH}}} ; k_{\text{rel}}^{\text{F,AmP}} = \frac{k'_{\text{F}}}{k'_{\text{HOH}}}$$

$$k_{\text{rel}}^{\text{amine}} = \frac{k_{\text{amine}}}{k_{\text{HOH}}} = \frac{(k_{\text{rel}}^{\text{F,ATP}}[\text{F}] - \frac{[\text{FPO}_3]}{[\text{HOPO}_3]}][\text{H}_2\text{O}])(k_{\text{rel}}^{\text{F,AmP}}[\text{F}] + [\text{H}_2\text{O}])}{([\text{HOPO}_3][\text{H}_2\text{O}] - k_{\text{rel}}^{\text{F,AmP}}[\text{F}])([\text{Amine}]}$$

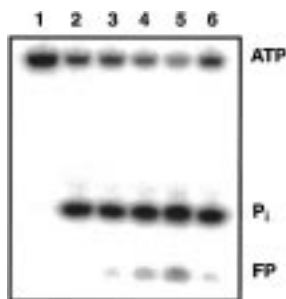
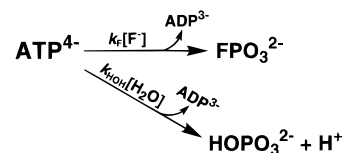


Figure 2. Fluoride trapping of phosphorylated amines resulting from nucleophilic attack with ATP. Radiolabeled ATP substrate and P_i and fluorophosphate (FP) products from single time points of several different reactions are separated on a representative polyacrylamide gel. The reactions were performed at 95 °C as described in the Experimental Section. Lane 1 contains ATP at time zero, and all other lanes correspond to a 360 min time point. Reaction of ATP in the absence of fluoride and amine nucleophiles, $[\text{FPO}_3]/[\text{HOPO}_3] = 0.000$ (lane 2); in the presence of 0.5 M fluoride, $[\text{FPO}_3]/[\text{HOPO}_3] = 0.014$ (lane 3); in the presence of 0.5 M fluoride and 1 M Im, $[\text{FPO}_3]/[\text{HOPO}_3] = 0.036$ (lane 4); in the presence of 0.5 M fluoride and 3 M Im, $[\text{FPO}_3]/[\text{HOPO}_3] = 0.076$ (lane 5); in the presence of 0.5 M fluoride and 1 M 2,6-dimethylpyridine, $[\text{FPO}_3]/[\text{HOPO}_3] = 0.015$ (lane 6).

and fluorophosphate products can be separated and quantitated by PAGE (see Experimental Section). The $[\text{FPO}_3]/[\text{HOPO}_3]$ product ratio increases with increasing Im (lanes 3, 4, and 5), presumably due to trapping of the unstable ImP product by reaction with fluoride. Consistent with this interpretation, the $[\text{FPO}_3]/[\text{HOPO}_3]$ product ratio is unaffected by the presence of 2,6-dimethylpyridine, a sterically hindered amine (lanes 3 and 6).⁹ The following section describes how rate constants for reactions of amines with ATP were determined via fluoride trapping (Scheme 3).

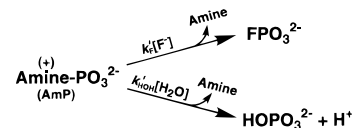
Fluoride Trapping To Measure Relative Rate Constants for Amine Reactions with ATP. The equation in Scheme 3 describes how $k_{\text{rel}}^{\text{amine}}$, the rate constant for reaction of ATP with each amine relative to that for reaction with water, is obtained. The $[\text{FPO}_3]/[\text{HOPO}_3]$ product ratio is a readout for the amount of transient phosphorylated amine and thus for $k_{\text{rel}}^{\text{amine}}$, but the contributions of two other rate constants to the product ratio must also be considered. The rate constant for reaction of ATP with fluoride relative to that for reaction with water, $k_{\text{rel}}^{\text{F,ATP}}$, describes the amount of fluorophosphate, if any, that arises from direct reaction of fluoride with ATP (Scheme 4). The rate constant for reaction of each phosphorylated amine with fluoride relative to that for reaction of water, $k_{\text{rel}}^{\text{F,AmP}}$, describes the

Scheme 4



$$k_{\text{rel}}^{\text{F,ATP}} = \frac{k_{\text{F}}}{k_{\text{HOH}}} = \frac{[\text{FPO}_3]}{[\text{HOPO}_3]} \times \frac{[\text{H}_2\text{O}]}{[\text{F}]}$$

Scheme 5



$$k_{\text{rel}}^{\text{F,AmP}} = \frac{k'_{\text{F}}}{k'_{\text{HOH}}} = \frac{[\text{FPO}_3]}{[\text{HOPO}_3]} \times \frac{[\text{H}_2\text{O}]}{[\text{F}]}$$

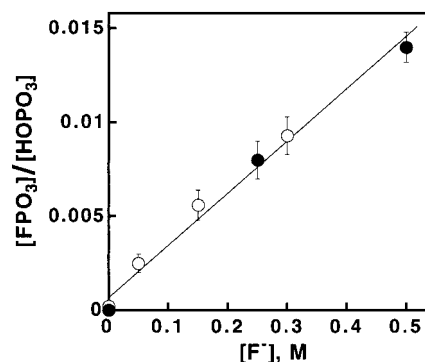


Figure 3. Dependence of the $[\text{FPO}_3]/[\text{HOPO}_3]$ product ratio on the concentration of fluoride nucleophile for reactions of ATP^{4-} . Reactions were performed at 95 °C and $I = 0.5$, and different symbols represent different buffer conditions: 30 mM sodium pyrophosphate, pH 8.3, and NaCl (●), or 30 mM tetramethylammonium phosphate, pH 8.0, and tetramethylammonium chloride (○). Error bars denote one standard deviation from the mean of four measurements, and the line is a least-squares fit to the combined data and gives a slope of 0.028 M^{-1} .

proportion of the phosphorylated amine that is trapped as fluorophosphate and not hydrolyzed to P_i (Scheme 5).

Scheme 4 highlights the part of Scheme 3 that is relevant for determining $k_{\text{rel}}^{\text{F,ATP}}$ and thus the amount of fluorophosphate produced from reaction of ATP and fluoride in the absence of amine. Varying concentrations of fluoride were added to reaction mixtures containing ATP, and surprisingly, based on previous reports that fluoride does not react with phosphate monoesters,¹⁹ fluorophosphate production was observed (see Discussion). The $[\text{FPO}_3]/[\text{HOPO}_3]$ product ratio was determined for these reactions, and the fluoride concentration dependence of this ratio is plotted in Figure 3. The slope of the line in Figure 3, representing the $[\text{FPO}_3]/[\text{HOPO}_3]$ ratio expected at 1 M fluoride, and the 55 M concentration of water in aqueous solution give $k_{\text{rel}}^{\text{F,ATP}} = 1.6$, according to the equation in Scheme 4.

Scheme 5 highlights the part of Scheme 3 that is relevant for determining $k_{\text{rel}}^{\text{F,AmP}}$ and thus the proportion of phosphorylated amine that is trapped as fluorophosphate and not hydrolyzed to P_i . For the phosphorylated pyridines, apparent second-order rate constants for reactions with fluoride (k'_F) were determined from k_{obs} as a function of fluoride concentration, and the apparent second-order rate constants for reactions with water

(19) Kirby, A. J.; Varvoglis, A. G. *J. Chem. Soc. (B)* **1968**, 135–141. Kirby, A. J.; Younas, M. *J. Chem. Soc. (B)* **1970**, 1165–1172.

Table 2. Apparent Second-Order Rate Constants for Reactions of Phosphorylated Amines with Fluoride and Water^a

phosphorylated amine	$k'_{\text{F}}, \text{M}^{-1} \text{s}^{-1}$ (fluoride)	$k'_{\text{HOH}}, \text{M}^{-1} \text{s}^{-1}$ (water)	$k_{\text{rel}}^{\text{F}, \text{Amp}}$ ($=k'_{\text{F}}/k'_{\text{HOH}}$)
pyridine	5.8×10^{-3}	2.3×10^{-4}	25
3-picoline	2.8×10^{-3}	8.2×10^{-5}	34
4-picoline	1.6×10^{-3}	3.3×10^{-5}	48
imidazole	4.2×10^{-5b}	1.6×10^{-6}	26

^a 30 mM sodium pyrophosphate, pH 8.3, $I = 0.5$ (NaCl). Reactions of phosphorylated pyridines were measured at 25 °C and reactions of ImP at 75 °C. k'_{F} and k'_{HOH} are apparent second-order rate constants for reactions with fluoride and water, respectively, as defined in Schemes 3 and 5. These rate constants are apparent because they are not necessarily pH-independent (see Experimental Section). ^b Calculated from $k_{\text{rel}}^{\text{F}, \text{Amp}} = k'_{\text{F}}/k'_{\text{HOH}}$ and $k'_{\text{HOH}} = 1.6 \times 10^{-6} \text{M}^{-1} \text{s}^{-1}$; k'_{HOH} is k_{obs} in the absence of fluoride divided by 55 M.

(k'_{HOH}) were determined from k_{obs} in the absence of added fluoride divided by 55 M water. Values of $k_{\text{rel}}^{\text{F}, \text{Amp}}$ were then calculated for each phosphorylated pyridine from the ratio of these rate constants, as defined in the equation in Scheme 5, and are reported in Table 2. For ImP, $k_{\text{rel}}^{\text{F}, \text{Amp}} (=26; \text{Table } 2)$ was obtained from the $[\text{FPO}_3]/[\text{HOPO}_3]$ product ratios from reactions containing radiolabeled ImP and several concentrations of fluoride, according to the equation in Scheme 5.

Finally, to obtain rate constants for reactions of amines with ATP, fluorophosphate production was monitored in reaction mixtures containing known concentrations of amine and fluoride. The relative rate constant with respect to water, $k_{\text{rel}}^{\text{amine}}$, for each amine could then be calculated from the $[\text{FPO}_3]/[\text{HOPO}_3]$ product ratio, $k_{\text{rel}}^{\text{F}, \text{ATP}} = 1.6$ (Figure 3), the appropriate $k_{\text{rel}}^{\text{F}, \text{Amp}}$ value (Table 2), and the concentrations of nucleophiles present ($[\text{F}^-]$, $[\text{Amine}]$, $[\text{H}_2\text{O}]$), as described in the equation in Scheme 3. Table 1 contains the data used to determine rate constants for individual amines, and the average rate constants are displayed in the second column from the right (average $k_{\text{rel}}^{\text{amine}}$). The deviations are rather large for several of the amines, and we attribute this to the sensitivity of the $k_{\text{rel}}^{\text{amine}}$ values to $[\text{FPO}_3]/[\text{HOPO}_3]$; there are uncertainties of $\pm 10\%$ in the measured ratios of $[\text{FPO}_3]/[\text{HOPO}_3]$, and small changes in these ratios have large effects on the calculated values of $k_{\text{rel}}^{\text{amine}}$. The estimated uncertainty of 2-fold in $k_{\text{rel}}^{\text{amine}}$ values does not affect the conclusions.

Second-Order Rate Constants for Amine Reactions with ATP. Despite our initial hesitance to interpret small increases in the rates of ATP disappearance upon addition of amines as signifying nucleophilic attack, we compared k_{amine} values that were obtained from these rate increases to k_{amine} values calculated in Table 1 from fluoride trapping experiments. Second-order rate constants of $k_{\text{amine}} = 9.0 \times 10^{-6}$, 11×10^{-6} , 8.5×10^{-6} , and $11 \times 10^{-6} \text{M}^{-1} \text{s}^{-1}$ for reactions at 95 °C of pyridine, 3-picoline, 4-picoline, and Im, respectively, were determined by plotting the values of k_{obs} in Table 1 as a function of amine concentration. These values are in reasonable agreement with the corresponding values of k_{amine} calculated from product ratios, differing by 15–40% (Table 3, 95 °C data vs Table 1, last column). Further, the sterically hindered amine 2,6-dimethylpyridine, which is not expected to react as a nucleophile with ATP, had no effect on the reaction rate. After these confirmations that the observed rate increases reflected nucleophilic reaction between ATP and amines, second-order rate constants were determined for reactions of amines and water with ATP at different temperatures (Table 3). As a further control, the values of $k_{\text{rel}}^{\text{amine}}$ for Im as a function of temperature were determined by product analysis in the presence of fluoride

(Table 3, bracketed values); these values are within 40% of those obtained by direct determination of rate effects and show the same trend with temperature. Activation parameters were calculated for the reactions of amines and water with ATP using the second-order rate constants measured at different temperatures (Table 3). Although there is considerable uncertainty in these activation parameters, they were used solely to extrapolate relative rate constants for comparisons below and in the Discussion.

Enzymatic Rate Enhancements. A nitrogen of histidine's Im ring is often a phosphate acceptor in biological phosphoryl transfer. Rate constants for the reaction of Im and ATP at physiological temperatures can be extrapolated using the activation parameters calculated in Table 3, facilitating comparison to analogous enzymatic reactions. For example, comparison of the extrapolated nonenzymatic rate constant of $2 \times 10^{-9} \text{M}^{-1} \text{s}^{-1}$ at 20 °C to the second-order rate constant of $\sim 10^6 \text{M}^{-1} \text{s}^{-1}$ for histidine phosphorylation by NDPK²⁰ reveals a 10^{15} -fold rate enhancement by this enzyme. Knowledge of the rate enhancements achieved by enzymes that use a histidine nucleophile to attack ATP allows calibration of individual catalytic contributions and comparison of the relative proficiencies of these enzymes.²¹

Discussion

Characterization of nonenzymatic reactions of ATP provides a starting point for dissection of enzyme-catalyzed reactions. Specifically, comparison of oxygen nucleophiles to nitrogen nucleophiles enables the nucleophilic catalysis model (see introduction and Figure 1) to be evaluated. In addition, the unexpected observation of the reaction of fluoride ion with ATP⁴⁻ calls into question the extent to which electrostatic repulsion influences phosphoryl transfer in aqueous solution. These points are considered below.

Nucleophilic Reactivity toward ATP⁴⁻. Examination of the relative rate constants ($k_{\text{rel}}^{\text{amine}}$) in Table 1 reveals that the amines investigated react with ATP ~ 10 -fold faster than does water at 95 °C. Different temperature dependencies for the reactions of amines and water with ATP were observed upon further analysis, with the relative rate constants with respect to water ($k_{\text{rel}}^{\text{amine}}$) increasing for each amine as temperature decreases (Table 3).

These results support the nucleophilic catalysis model depicted in Figure 1B. The rate constants for the amine reactions studied exceed that for the water reaction by 30–100-fold at the physiological temperature of 37 °C, values obtained by extrapolation using the activation parameters in Table 3. The larger rate constants of the amine reactions suggest that the overall reaction of ATP with an oxygen nucleophile can be accelerated by the intermediacy of an amine nucleophile and the subsequent breakdown of the unstable amine phosphate product (Figure 1B).

Histidine Nucleophiles in Enzymatic Phosphoryl Transfer from ATP. Applying the chemical perspective obtained from kinetic comparison of oxygen and nitrogen nucleophiles toward ATP, it appears that enzymes such as NDPK may exploit the 30–100-fold greater reactivity of amine nucleophiles in catalysis (Figure 1B). It is likely that enzymes are able to further increase the reactivity differences between classes of nucleophiles by

(20) Schaertl, S.; Konrad, M.; Geeves, M. A. *J. Biol. Chem.* **1998**, *273*, 5662–5669. Schneider, B.; Xu, Y. W.; Sellam, O.; Sarfati, R.; Janin, J.; Véron, M.; Deville-Bonne, D. *J. Biol. Chem.* **1998**, *273*, 11491–11497.

(21) See, for example: Radzicka, A.; Wolfenden, R. *Science* **1995**, *267*, 90–93.

Table 3. Temperature Dependence of Second-Order Rate Constants ($M^{-1} s^{-1}$) for Reactions of ATP with Water and Amines^a

$T, ^\circ C$	water		pyridine		3-picoline		4-picoline		imidazole	
	$10^6 k_{HOH}$	k_{rel}	$10^6 k_{amine}$	k_{rel}^{amine}	$10^6 k_{amine}$	k_{rel}^{amine}	$10^6 k_{amine}$	k_{rel}^{amine}	$10^6 k_{amine}$	k_{rel}^{amine}
95	1.1	(1)	9.0	8	11	10	8.5	8	11	10 [7]
85	0.33	(1)	3.7	11	3.5	11	3.8	12	4.0	12 [9]
75	0.11	(1)	1.4	13	1.2	11	1.4	13	1.6	15 [12]
65	0.033	(1)	0.50	15	0.65	20	0.88	27	0.52	16 [15]
$\Delta H^\ddagger,^b$ kcal/mol	28		23		23		19		24	
$\Delta S^\ddagger,^b$ eu	-3		-5		-5		-8		-4	

^a 30 mM sodium pyrophosphate, pH 8.3, and $I = 0.5$ (NaCl). Rate constants are defined in Scheme 3. Note that these rate constants were obtained by direct determination of rate effects, rather than by product analysis with added fluoride as in Table 1. Relative rate constants are unitless. Relative rate constants for reactions of Im were also obtained by the product analysis method for comparison and are shown in brackets. ^b Calculated from $k/T = (k_B/h) \exp(\Delta S^\ddagger/R) \exp[-\Delta H^\ddagger/(RT)]$.

altering the active site environment, thereby enhancing nucleophilic catalysis. Other factors, in addition to this kinetic advantage, almost certainly contribute to the use of histidine nucleophiles in biological phosphoryl transfer, and several of these factors are discussed below.

The intermediacy of phosphorylated histidine in the NDPK reaction is an example of the principle of economy in the evolution of binding sites, an evolutionary strategy first noted by Frey and co-workers.²² Instead of evolving functionally analogous binding sites for the two nucleotides involved in this symmetric reaction, the enzyme has evolved a means of catalyzing the overall reaction with just one binding site. This evolutionary rationale for the NDPK mechanism accounts for the use of a covalent nucleophile by the enzyme, and the kinetic advantage of amine nucleophiles may account for the specific use of a covalent histidine nucleophile. In contrast to the NDPK mechanism, adenylate kinase produces two ADP molecules via direct nucleophilic attack of AMP upon ATP, without a phosphorylated intermediate. Although NDPK and adenylate kinase catalyze chemically equivalent reactions, the asymmetry of the adenylate kinase reaction is not conducive to an economy of binding sites.²²

The covalent participation of histidine rather than another nucleophilic amino acid in the NDPK reaction may be related to the kinetic advantage described above, but it could also or instead be thermodynamic in origin. The overall NDPK reaction conserves an unstable phosphoanhydride bond, and intermediate phosphorylation of histidine maintains the phosphate in a kinetically labile and thermodynamically unstable linkage. Figure 4 (solid line) depicts the free energy profile for the nonenzymatic reactions that correspond to the NDPK reaction scheme. The similar energy levels of the wells corresponding to the ATP substrate, the ImP intermediate, and the NTP product indicate that these compounds have similar stabilities, and the transition state barriers for the steps are similar.

In contrast, phosphorylation of a serine or threonine alcohol nucleophile of NDPK would trap the phosphate in an ester linkage that is kinetically and thermodynamically stable relative to a phosphoanhydride bond. Figure 4 (dashed line) depicts the free energy profile for the nonenzymatic reactions that correspond to the reaction scheme of a hypothetical NDPK with an alcohol nucleophile. The hypothetical phosphoenzyme intermediate (ROP) is ~ 6.5 kcal/mol more stable than ATP and NTP, and there is also a larger kinetic barrier for reaction of the phosphorylated alcohol than for ImP. Thus, a phosphorylated alcohol intermediate would tend to accumulate in the hypothetical NDPK reaction, based on thermodynamic and kinetic parameters for phosphorylated alcohols in solution.

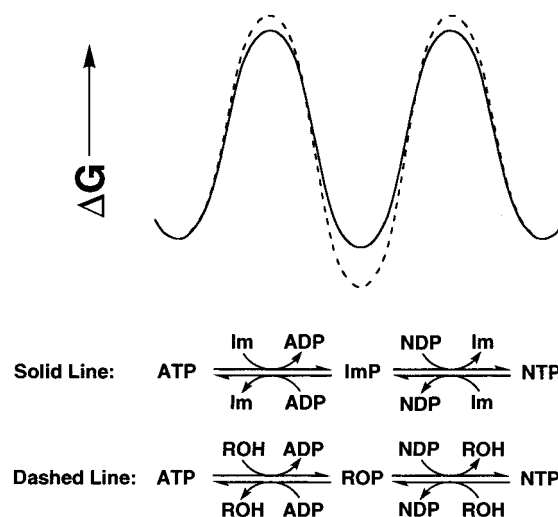


Figure 4. Comparison of ImP and phosphorylated alcohols as intermediates in overall phosphoryl transfer from ATP to an NDP at 25 °C and pH 7.4. Equilibrium and rate constants used to calculate free energies are described in the Experimental Section, and free energies are drawn to scale. The solid line represents the free energy profile for intermediate phosphorylation of Im, which is described by the upper reaction scheme. The dashed line represents the free energy profile for intermediate phosphorylation of an alcohol (ROH) to form a phosphorylated alcohol (ROP), which is described by the lower reaction scheme.

Intermediate phosphorylation of tyrosine, cysteine, aspartate, or glutamate, like phosphorylation of histidine, would be expected to maintain phosphate in a linkage that is labile and unstable relative to the phosphoanhydride bond of ATP. The kinetic advantage of amine nucleophiles may have favored selection of histidine as an alternative to these enzymatic nucleophiles in the NDPK reaction.

Although kinetic and thermodynamic advantages conferred by the histidine nucleophile both appear to justify its use in the NDPK reaction, kinetic advantages are expected to be less important in some enzymatic contexts. The histidine kinases of histidyl-aspartyl phosphorelays autophosphorylate a specific histidine en route to phosphorylating an aspartate of a response regulator.² However, it is doubtful that the histidine nucleophile of the kinase component has been selected due to its intrinsic reactivity toward ATP. The combination of the phosphorylation partners histidine and aspartate in these signal transduction pathways can instead be rationalized thermodynamically. Intermediate phosphorylation of histidine maintains the phosphate in a kinetically labile and thermodynamically unstable linkage for subsequent transfer to aspartate. By requiring phosphorylated histidine as a phosphodonor for aspartate rather than simply phosphorylating the aspartate of the response regulator directly,

(22) Sheu, K. R.; Richard, J. P.; Frey, P. A. *Biochemistry* **1979**, *18*, 5548–5556. Frey, P. A. *Adv. Enzymol.* **1989**, *62*, 119–201. See also: Hanson, K. R.; Rose, I. A. *Acc. Chem. Res.* **1975**, *8*, 1–10.

histidyl-aspartyl phosphorelays have installed an additional regulatory checkpoint.²³ In contrast to the instability of phosphohistidine, which makes it an apt phosphodonator, phosphoserine and phosphothreonine are intrinsically stable. This stability enables the phosphorylation-induced conformational changes that are characteristic of signal transduction to be sustained and may account for the ubiquity of serine and threonine kinases in phosphorylation cascades.²⁴

Our results suggest that reactivity is one component that may have favored the participation of histidine in some phosphoryl transfer reactions, and thermodynamic factors may also have contributed to this outcome. Nevertheless, amine catalysis is only one of a multitude of solutions to the problem of biological phosphoryl transfer, and the potential advantages of a histidine nucleophile are affected by specific active site contexts and functional requirements. For example, despite the kinetic and thermodynamic stability of phosphorylated alcohols in solution, alkaline phosphatase is one of a group of catalytically proficient enzymes that exploit them as intermediates. The Zn^{2+} ions in the alkaline phosphatase active site may compensate for the apparent disadvantages of its phosphoserine intermediate relative to phosphohistidine; Zn^{2+} is thought to activate the serine nucleophile for formation of the phosphoserine intermediate and then stabilize the serine as a leaving group during hydrolysis of this intermediate.²⁵ The transition-state stabilization provided by this metal ion is presumably not available to enzymes that proceed via phosphohistidine intermediates because nitrogen nucleophiles lack the additional lone pair of electrons required for simultaneous nucleophilic attack and interaction with a metal ion. Furthermore, many of alkaline phosphatase's potential substrates are low-energy phosphate esters that are similar in stability to phosphoserine, so trapping of the intermediate in a thermodynamic well, as discussed above for a hypothetical NDPK, may not be a factor. Analogous mechanistic opportunities or functional requirements have presumably affected the selection of nucleophiles used by other phosphoryl transfer enzymes. In addition, the stochastic nature of natural selection and the protein templates already available are likely to have influenced the ultimate catalytic mechanism.²⁶

Electrostatic Repulsion of Anionic Nucleophiles? Electrostatic repulsion of anionic nucleophiles by the negative charges of ATP^{4-} and phosphate monoester dianions has been suggested to slow their reactions relative to reactions of uncharged nucleophiles.²⁷ We were therefore surprised to observe in control reactions for the fluoride trapping experiments that the anionic nucleophile fluoride reacts with ATP^{4-} with $k_{rel}^{F^-,ATP} = 1.6$ (Figure 3), similar to k_{rel} values measured for the uncharged oxygen and nitrogen nucleophiles surveyed (Figure 5). Data for reactions of ATP^{4-} with alcohols, pyridines, Im, and fluoride are combined in Figure 5. Although these nucleophiles are not structurally homologous to each other and are therefore not

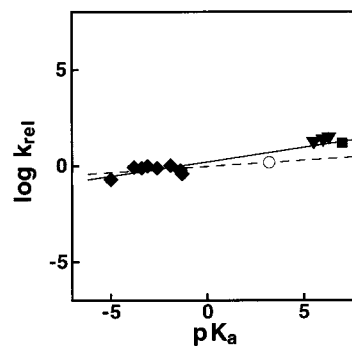


Figure 5. Dependence of the rate constants for the reactions of nucleophiles with ATP^{4-} on the pK_a of the nucleophile. Relative rate constants for reactions of fluoride (○), Im (■), and pyridines (▼) are from this work and were measured at 65 °C and $I = 0.5$. Relative rate constants for reactions of alcohols (◆) are from ref 16 and were measured at 60 °C and $I = 0.1$. The pK_a values used in the plot are for the conjugate acid of the nucleophile. The solid line of slope 0.15 is a least-squares fit to all of the data for this nonhomologous series of nucleophiles and is included solely for comparison. The dashed line is a least-squares fit to the alcohol data and gives $\beta_{nucleophile} = 0.07$.¹⁶ The relative rate constant for reaction of fluoride ion with ATP^{4-} does not deviate significantly from either linear correlation.

expected to follow the same linear free energy correlation, there is no indication of a large negative deviation for the negatively charged fluoride ion.

Detection of the reaction of fluoride ion with ATP^{4-} led us to revisit earlier reports that fluoride ion does not react with phosphate monoester dianions.¹⁹ We did observe a fluorophosphate product by ^{31}P NMR in reaction mixtures containing fluoride and $PNPP^{2-}$ (see Experimental Section), suggesting that reaction does, indeed, occur between these anions. The previous conclusion relied on an indirect assay, detecting potential fluorophosphate product by monitoring a decrease in the final amount of P_i , and could easily have missed the less than 10% fluorophosphate product observed in the NMR experiments. The $k_{rel}^{F^-,PNPP}$ value of 2 ± 1 determined from our NMR analysis indicates that the rate constant for reaction of fluoride with $PNPP^{2-}$ is not significantly different from the second-order rate constant for reaction of water with $PNPP^{2-}$. Furthermore, the k_{rel} values for reaction of fluoride ion with $PNPP^{2-}$ and ATP^{4-} ($k_{rel}^{F^-,ATP} = 1.6$) are similar, despite the difference in charge between these compounds.

Several models can account for nucleophilic attack of ATP^{4-} by fluoride ion. It is possible that fluoride is an intrinsically more reactive nucleophile toward ATP than is indicated by its rate constant, but that its high reactivity is repressed due to electrostatic repulsion. Alternatively, the sodium counterion could coordinate the reactive phosphoryl groups and the nucleophilic fluoride ion, overcoming unfavorable effects from electrostatic repulsion by bridging them together.²⁸ However, substitution of the sodium counterion by tetramethylammonium has no effect on the reactivity of fluoride ion relative to water (Figure 3), providing no evidence for bridging of the substrates by sodium. Another possibility is that the charge repulsion is screened at the high ionic strength of these reactions ($I = 0.5$). However, varying the ionic strength between 0.05 and 1 M also had no effect on the reactivity of fluoride ion relative to water (data not shown). Finally, it is possible that electrostatic repulsion has little effect on the reaction of fluoride with ATP in aqueous solutions of moderate ionic strength. This provides the simplest model to account for all of the data observed herein.

(23) Appleby, J. L.; Parkinson, J. S.; Bourret, R. B. *Cell* **1996**, *86*, 845–848. Grossman, A. D. *Annu. Rev. Genet.* **1995**, *29*, 477–508.

(24) Stock, J. B.; Stock, A. M.; Mottonen, J. M. *Nature* **1990**, *344*, 395–400. Stock, J. B.; Lukat, G. S. *Annu. Rev. Biophys. Biophys. Chem.* **1991**, *20*, 109–136.

(25) Hengge, A. C. In *Comprehensive Biological Catalysis: A Mechanistic Reference*; Sinnott, M., Ed.; Academic Press: San Diego, CA, 1998; Vol. 1, pp 517–542.

(26) For review, see: O'Brien, P. J.; Herschlag, D. *Chem. Biol.* **1999**, *6*, R91–R105.

(27) Kirby, A. J.; Jencks, W. P. *J. Am. Chem. Soc.* **1965**, *87*, 3209–3216. Kirby, A. J.; Younas, M. *J. Chem. Soc. B* **1970**, 1165–1172. Westheimer, F. H. *Science* **1987**, *235*, 1173–1177. Abeles, R. H.; Frey, P. A.; Jencks, W. P. *Biochemistry*; Jones and Bartlett: Boston, 1992; pp 295–328. Lehninger, A. L. *Biochemistry*, 2nd ed; Worth Publishers: New York, 1978; pp 387–416.

(28) Herschlag, D.; Jencks, W. P. *J. Am. Chem. Soc.* **1986**, *108*, 7938–7946.

Previous studies of reactions of anionic nucleophiles with phosphorylated compounds support the latter model and suggest that the apparent absence of electrostatic repulsion noted above is not specific to special properties of fluoride.²⁹ Rate constants for the reactions of anionic oxygen nucleophiles with the monoanions of methyl 2,4-dinitrophenyl phosphate and phosphorylated 4-picoline were compared with those for the corresponding reactions of pyridinium-*N*-sulfonate and acetyl chloride, which have no net charge. No large deviations were observed when the rate constants for reactions of nucleophiles

(29) Herschlag, D.; Jencks, W. P. *J. Am. Chem. Soc.* **1989**, *111*, 7587–7596.

(30) Reactions of fluoride ion with phosphorylated compounds other than ATP⁴⁻ and PNPP²⁻ have previously been observed. Second-order rate constants for reactions of fluoride ion and other anionic nucleophiles with the uncharged triester, the monoanionic diester, and the dianionic monoester of 2,4-dinitrophenyl phosphate have been compared (Kirby, A. J.; Younas, M. J. *Chem. Soc. (B)* **1970**, 1165–1172). The decrease in rate constants in going from the uncharged triester to the monoanionic diester to the dianionic monoester was interpreted to represent an increase in electrostatic repulsion with increasing charge on the phosphoryl group. This interpretation is problematic, however, because in addition to the different charges on the phosphoryl groups of these esters, reactions of these compounds exhibit different amounts of nucleophilic involvement in their respective transition states. Thus, the observed differences in rate constants may reflect differences in intrinsic reactivities of the phosphate esters that arise from features distinct from electrostatic repulsion (see ref 29 for a more detailed discussion). Reactions of fluoride ion with phosphoramidate (Jencks, W. P.; Gilchrist, M. J. *Am. Chem. Soc.* **1965**, *87*, 3199–3209) and acetyl phosphate (DiSabato, G.; Jencks, W. P. *J. Am. Chem. Soc.* **1961**, *83*, 4393–4400) have also been observed. Crude measurements suggest that the rate constant for reaction of fluoride (relative to water) with neutral phosphoramidate is larger than that for reaction of fluoride (again relative to water) with monoanionic phosphoramidate; similarly, the relative rate constant for the reaction of fluoride with the acetyl phosphate monoanion is larger than the upper limit obtained for the relative rate constant for the reaction of fluoride with the acetyl phosphate dianion. However, the reactions of these species may also involve different amounts of nucleophilic participation in the transition state, again limiting the applicability of these results to the question of electrostatic repulsion.

of varying charge type with the phosphorylated electrophiles were compared with those for reactions with the uncharged electrophiles.²⁹ The absence of large deviations suggests that reactions of anionic nucleophiles with anionic phosphorylated compounds are not significantly inhibited by electrostatic repulsion. The only relative rate data that we are aware of in support of the previous suggestions that electrostatic repulsion substantially inhibits phosphoryl transfer to anions may instead reflect differences in the intrinsic reactivities of the phosphate esters used in those comparisons.³⁰

In conclusion, there is no indication that electrostatic repulsion affects the reactivity of the anionic nucleophile fluoride toward ATP in aqueous solution, and no compelling reason to invoke electrostatic repulsion for reactions of other anions with ATP. Although enzyme active sites must be designed to accommodate these highly charged reactants and electrostatic stabilization is indisputably a central feature of enzymatic catalysis, the apparent absence of repulsion between fluoride and ATP challenges the distinct idea that enzymes catalyze phosphoryl transfer by overcoming electrostatic repulsion that hinders reaction between anions in aqueous solution.

Acknowledgment. This work was supported by a Packard Fellowship in Science and Engineering to D.H. S.J.A. is a Howard Hughes Medical Institute Predoctoral Fellow. Purified H122G NDPK was a kind gift from Benoit Schneider and Dominique Deville-Bonne of the Institut Pasteur. We are grateful to members of the Herschlag laboratory for comments on the manuscript.

JA990903W